Supporting Information for Moerman et al., 2014 (doi:10.1002/2014GL061696)

Meteoric water lines

The Mulu local meteoric water line (LMWL; $\delta D = 7.9*\delta^{18}O + 10.3$), calculated from all daily rainfall isotopic samples presented in this study, is nearly identical to the global meteoric water line (GMWL; $\delta D = 8*\delta^{18}O + 10$ from *Craig* [1961]), suggesting that sub-cloud evaporation of rainfall is limited (Figure S2). Dripwater $\delta^{18}O$ vs. δD from all three drip sites plots slightly to the left of the Mulu LMWL, suggesting the possible contribution of recycled soil moisture [*Gat et al.*, 1994] or cave-surface condensates [*Genty et al.*, 2014] to seepage waters feeding WF, WS, and L2.

Stalagmite forward model development

To investigate how ENSO variability may be recorded in Borneo speleothem $\delta^{18}O$, we generate pseudo-stalagmites of varying growth rates that reflect ENSO-related dripwater $\delta^{18}O$ variability in drips WS and L2. We perform a peak-to-peak linear regression of Mulu dripwater $\delta^{18}O$ onto sea surface temperature (SST) anomalies in the NINO3.4 index by relating the maximum (minimum) dripwater $\delta^{18}O$ value between October – May during the 2006/2007 and 2009/2010 El Niño events (2007/2008 and 2010/2011 La Niña events) to maximum NINO3.4 SST anomalies for each event (Figure S5a). We do not include the weak 2008/2009 La Niña in this calibration due to the influence of persistent enhanced intraseasonal variability. Inclusion of this data point considerably reduces the correlation between NINO3.4 and dripwater $\delta^{18}O$ (Figure S5b). We apply this calibration to the NINO3.4 extended index [*Kaplan et al.*, 1998] to obtain pseudo-dripwater $\delta^{18}O$ timeseries spanning 1856-2013. To generate speleothem $\delta^{18}O$, we smooth the pseudo-dripwater $\delta^{18}O$ timeseries with 1-yr, 10-yr, and 40-yr running means,

representing different growth rates. As we are only interested in comparing relative $\delta^{18}O$ differences, we do not incorporate temperature-dependent water-to-calcite fractionation into this simple model. We also assume constant cave temperature.

Attribution analysis for mean $\delta^{18}O$ offsets between pseudo-stalagmites

To constrain the sources likely responsible for creating the ~0.8‰ offset in mean $\delta^{18}O$ between the WS and L2 pseudo-stalagmites, we utilize our dripwater forward model to generate pseudo-stalagmites from different versions of modeled dripwater $\delta^{18}O$ (Figure S5c) and thus isolate potential influences – namely different residence times, contributions from well-mixed reservoirs, and precipitation amount-weighting. The variability in the observed L2 dripwater $\delta^{18}O$ timeseries, and thus the pseudo-stalagmite generated from it, is the product of two vadose zone reservoirs: (1) Reservoir A, which has with a residence time of ~10 months that is recharged autogenically, and (2) Reservoir B, which has a significantly longer residence time. Therefore, to differentiate the impact of these two influences on the mean $\delta^{18}O$ of pseudo-stalagmite L2, we isolate the contribution of Reservoir A by generating a pseudo-stalagmite reflecting modeled L2 dripwater d18O variability only with a 10-month residence time simulated using the autogenic recharge model, which we refer to as $L2_{res\text{-}A}$. The mean $\delta^{18}O$ value of pseudo-stalagmite $L2_{res\text{-}A}$ differs from that of pseudo-stalagmite L2 by only ~ 0.1‰, suggesting that the impact of Reservoir B on pseudo-stalagmite L2 mean $\delta^{18}O$, and thus the offset with pseudo-stalagmite WS, is limited and that difference in residence time is likely a major influence.

Next, we investigate the role of precipitation amount-weighting by creating WS and L2 pseudo-stalagmites from non-amount-weighted modeled dripwater $\delta^{18}O$ timeseries with 4-month

and 10-month residence times, respectively, referred to as $WS_{non\text{-}aw}$ and $L2_{non\text{-}aw}$. Whereas mean $\delta^{18}O$ for pseudo-stalagmite L2 is 0.75‰ heavier than $L2_{non\text{-}aw}$, mean $\delta^{18}O$ for pseudo-stalagmite WS is only 0.45‰ heavier than $WS_{non\text{-}aw}$ (Figure S6). The unequal influence of amount-weighting on the isotopic composition of WS versus L2 thus contributes ~ 0.3‰ to the mean offset between pseudo-stalagmite WS and L2. The variable effect of amount-weighting on WS versus L2 dripwater $\delta^{18}O$ is illustrated in Figure S7. While WS dripwater $\delta^{18}O$ modeled with amount-weighting is more depleted during La Niña events than when modeled without amount-weighting, as expected, amount-weighted L2 dripwater $\delta^{18}O$ is more depleted across the entire timeseries likely due to enhanced mixing given its longer residence time. As a result, the overall mean of amount-weighted L2 dripwater $\delta^{18}O$ is more negative than that for amount-weighted WS.

Based on this attribution analysis, we conclude that the majority of the ~0.8‰ offset in mean $\delta^{18}O$ between pseudo-stalagmites WS and L2 can be attributed to the interaction of asymmetry in ENSO extremes, variable residence times, and precipitation amount-weighting. It is important to note this offset in the pseudo-stalagmites is similar to actual mean $\delta^{18}O$ offsets of up to ~0.7‰ observed between Borneo stalagmite records [*Partin et al.*, 2007; *Carolin et al.*, 2013].

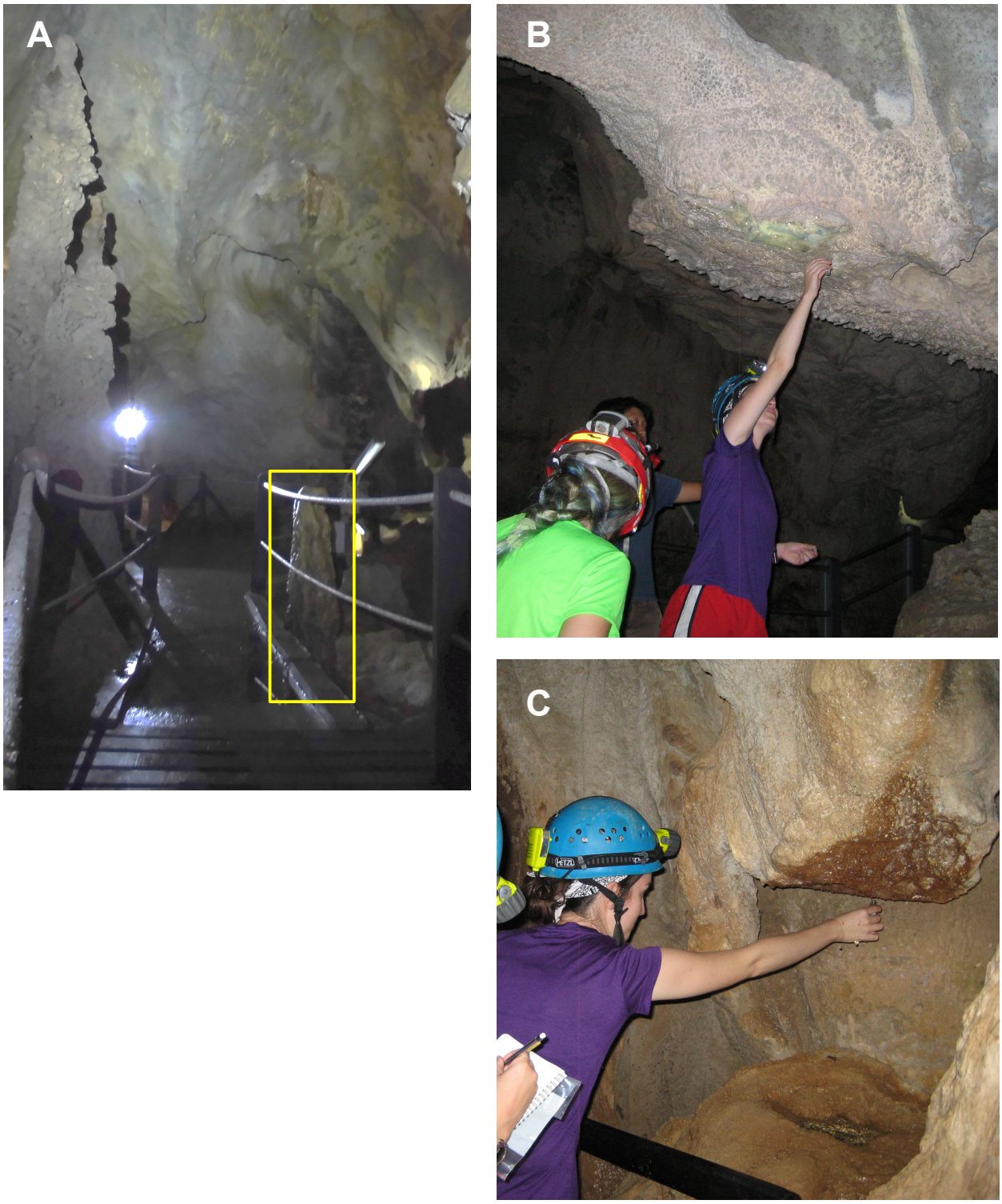

Figure S1
Photos of timeseries drip sites (a) L2, (b) WS, and (WF). Note that WS drips onto detrital bedrock.

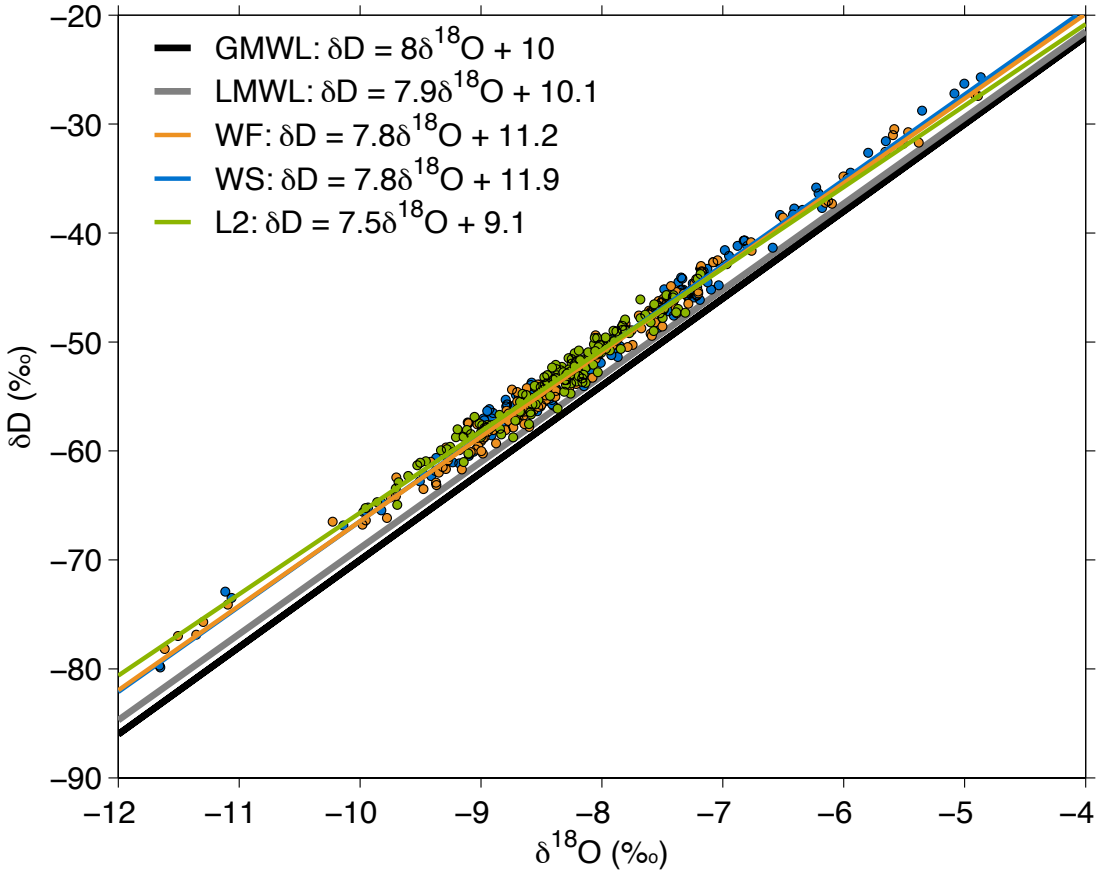

Figure S2
Comparison of timeseries drip $\delta^{18}O$/ δD plots with Mulu LMWL (gray line; this study) and GMWL [black line; *Craig*, 1961]. Individual dripwater $\delta^{18}O$ versus δD values are plotted as orange circles for WF, blue circles for WS, and green circles for L2. Water lines for drips WF, WS, and L2 are shown as orange, blue, and green lines respectively.

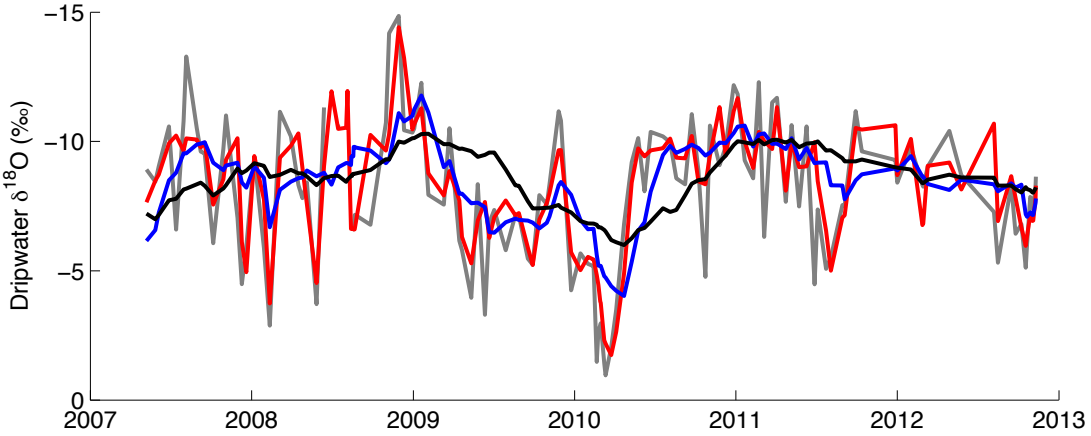

Figure S3
Selected modeled dripwater $\delta^{18}O$ timeseries generated by inputting daily amount-weighted Mulu rainfall $\delta^{18}O$ into the autogenic recharge model and applying an averaging interval of two weeks (gray), one month (red), three months (blue), and nine months (black).

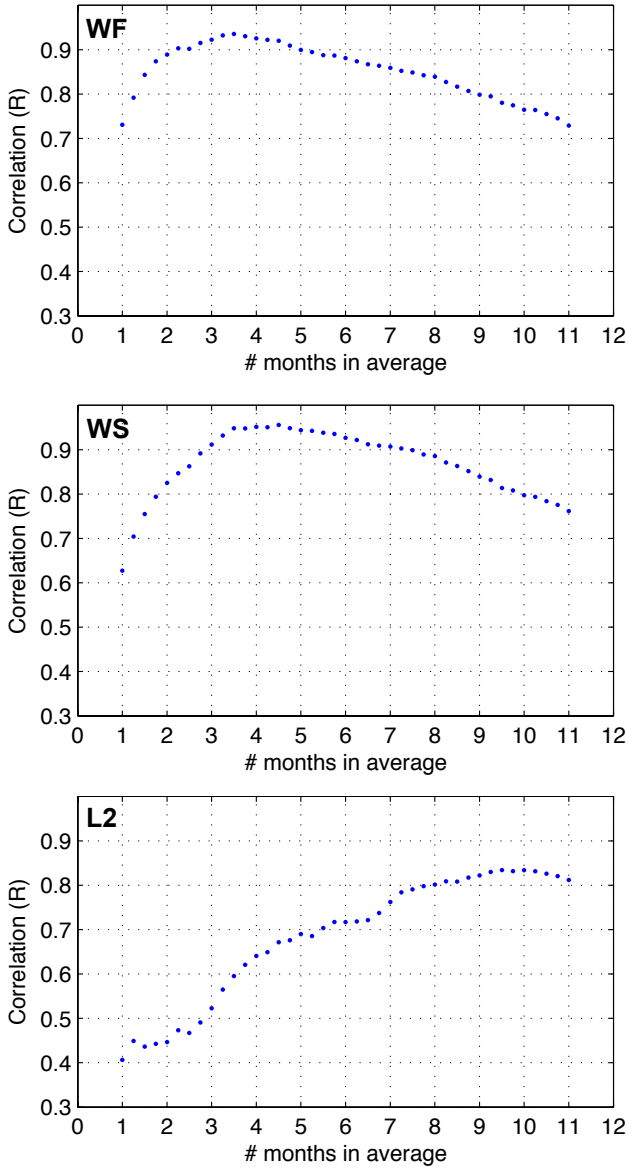

Figure S4
Correlation between observed and modeled Mulu dripwater $\delta^{18}O$ plotted against corresponding averaging interval used in the autogenic recharge model to generate modeled dripwater $\delta^{18}O$ with different residence times.

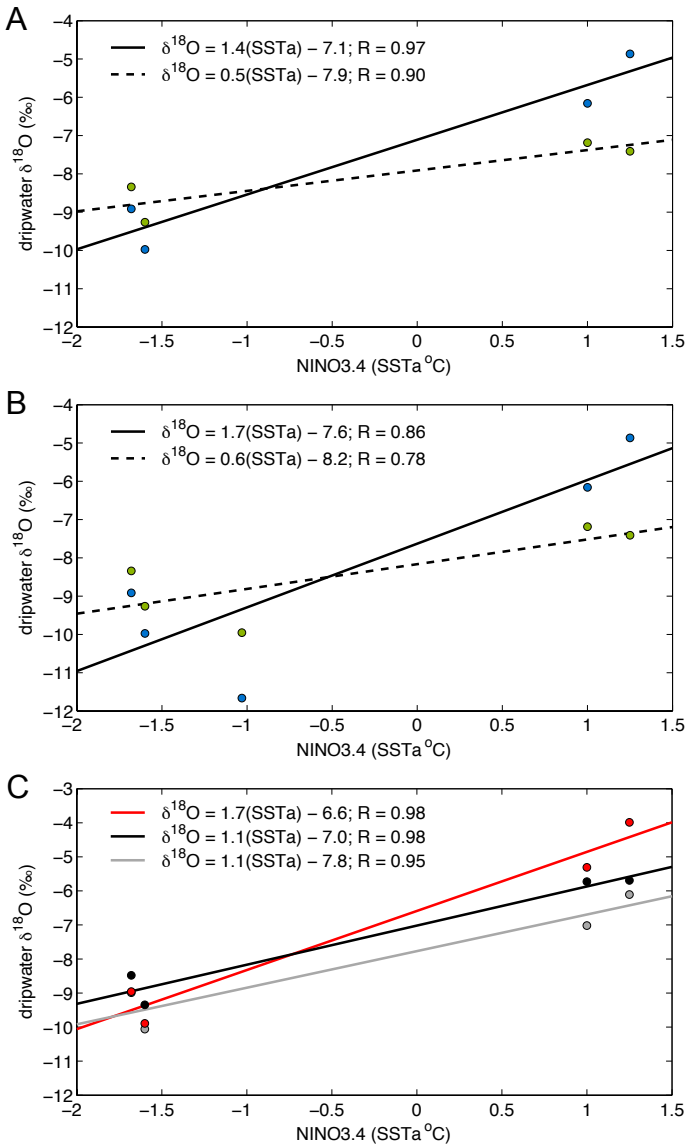

Figure S5
Maximum dripwater $\delta^{18}O$ anomalies between October-May during ENSO events regressed onto maximum sea surface temperature anomalies (SSTa) in the NINO3.4 region across specified time periods. (a) Observed WS (blue circles) and L2 (green circles) dripwater $\delta^{18}O$ maximum anomalies for 2006/2007 and 2009/2010 El Niño and 2007/2008 and 2010/2011 La Niña events. Lines represent regression equations for WS (solid) and L2 (dashed). (b) same as (a) but includes 2007/2008 weak La Niña event. (c) same as (a) but for modeled dripwater $\delta^{18}O$ maximum anomalies (circles) and regression equations (lines) for amount-weighted modeled L2 dripwater $\delta^{18}O$ with a 10-month residence time (gray), non-amount-weighted modeled L2 dripwater $\delta^{18}O$ with a 10-month residence time (black), and non-amount-weighted modeled WS dripwater $\delta^{18}O$ with a 4-month residence time (red).

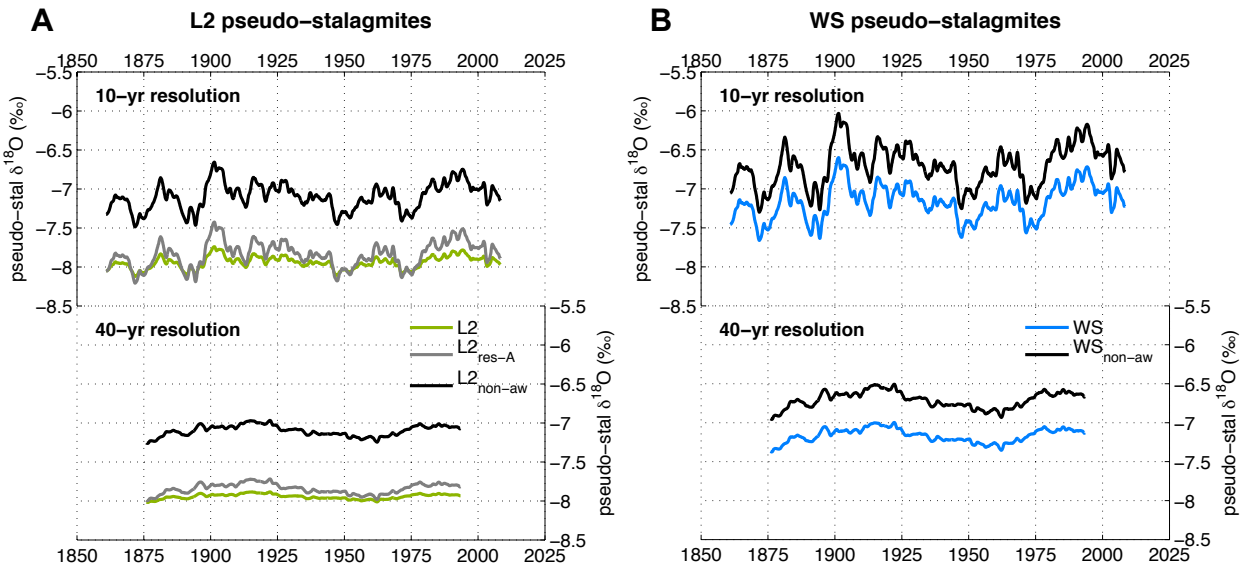

Figure S6
Pseudo-stalagmite $\delta^{18}O$ timeseries generated from the peak-to-peak relationship between the NINO3.4 index and observed and modeled dripwater $\delta^{18}O$ timeseries. (a) L2 pseudo-stalagmite timeseries with a 10-year (top panel) and 40-year (bottom panel) sampling resolution generated from observed L2 dripwater $\delta^{18}O$ (green), amount-weighted L2 dripwater $\delta^{18}O$ modeled with an ~10-month residence time (gray), and non-amount-weighted L2 dripwater $\delta^{18}O$ modeled with an ~10-month residence time (black). (b) same as (a) but for WS pseudo-stalagmite timeseries generated from observed WS dripwater $\delta^{18}O$ (blue) and non-amount-weighted WS dripwater $\delta^{18}O$ modeled with an ~4-month residence time (black). All modeled dripwater $\delta^{18}O$ timeseries used to generate pseudo-stalagmites are simulated using the autogenic recharge model fed by a single reservoir with the specified residence time.

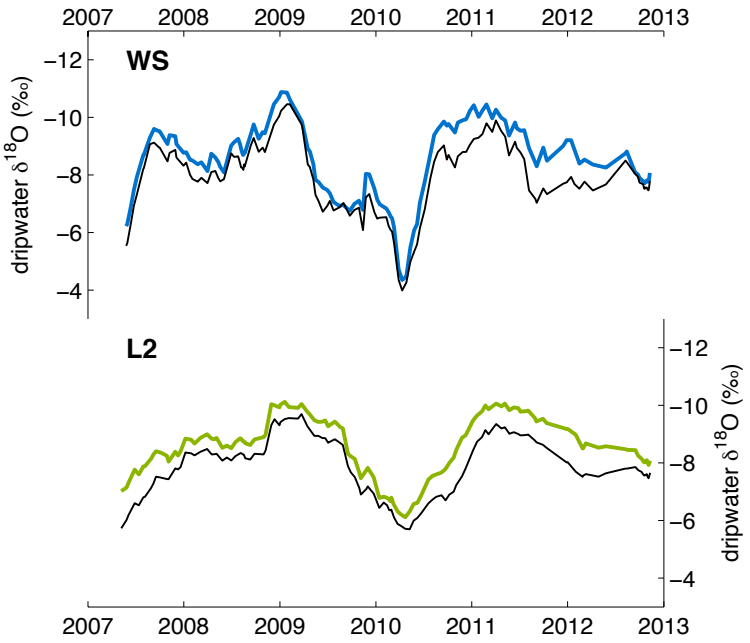

Figure S7
Amount-weighted versus non-amount-weighted dripwater $\delta^{18}O$ timeseries modeled using the autogenic recharge model. (top) WS dripwater $\delta^{18}O$ timeseries modeled with a 4-month residence time with amount-weighting (blue) and without amount-weighting (black). (bottom) same as (top) but for L2 dripwater $\delta^{18}O$ timeseries modeled with a 10-month residence time and amount-weighting plotted in green.

References

Carolin, S. A., K. M. Cobb, J. F. Adkins, B. Clark, J. L. Conroy, S. Lejau, J. Malang, and A. A. Tuen (2013), Varied response of western Pacific hydrology to climate forcings over the last glacial period, *Science*, *340*(6140), 1564-1566.

Craig, H. (1961), Isotopic variations in meteoric waters, *Science*, *133*(346), 1702-&.

Gat, J. R., C. J. Bowser, and C. Kendall (1994), The contribution of evaporation from the great-lakes to the continental atmosphere - estimate based on stable-isotope data, *Geophys. Res. Lett.*, *21*(7), 557-560.

Genty, D., et al. (2014), Rainfall and cave water isotopic relationships in two South-France sites, *Geochim. Cosmochim. Acta*, *131*, 323-343.

Kaplan, A., M. A. Cane, Y. Kushnir, A. C. Clement, M. B. Blumenthal, and B. Rajagopalan (1998), Analyses of global sea surface temperature 1856-1991, *Journal of Geophysical Research-Oceans*, *103*(C9), 18567-18589.

Partin, J. W., K. M. Cobb, J. F. Adkins, B. Clark, and D. P. Fernandez (2007), Millennial-scale trends in west Pacific warm pool hydrology since the Last Glacial Maximum, *Nature*, *449*(7161), 452-455.